

UCSF

UC San Francisco Previously Published Works

Title

Adenomatoid tumors of the male and female genital tract are defined by TRAF7 mutations that drive aberrant NF- κ B pathway activation.

Permalink

<https://escholarship.org/uc/item/1c16x60x>

Journal

Modern pathology : an official journal of the United States and Canadian Academy of Pathology, Inc, 31(4)

ISSN

0893-3952

Authors

Goode, Benjamin
Joseph, Nancy M
Stevens, Meredith
et al.

Publication Date

2018-04-01

DOI

10.1038/modpathol.2017.153

Peer reviewed



Published in final edited form as:

Mod Pathol. 2018 April ; 31(4): 660–673. doi:10.1038/modpathol.2017.153.

Adenomatoid tumors of the male and female genital tract are defined by *TRAF7* mutations that drive aberrant NF- κ B pathway activation

Benjamin Goode¹, Nancy M. Joseph^{1,2}, Meredith Stevers¹, Jessica van Ziffle^{1,2}, Courtney Onodera², Eric Talevich², James P. Grenert^{1,2}, Iwei Yeh^{1,2}, Boris C. Bastian^{1,2}, Joanna J. Phillips^{1,3}, Karuna Garg¹, Joseph T. Rabban¹, Charles Zaloudek¹, and David A. Solomon^{1,2}

¹Department of Pathology, University of California, San Francisco, CA, United States

²Clinical Cancer Genomics Laboratory, University of California, San Francisco, CA, United States

³Department of Neurological Surgery, University of California, San Francisco, CA United States

Abstract

Adenomatoid tumors are the most common neoplasm of the epididymis, and histologically similar adenomatoid tumors also commonly arise in the uterus and fallopian tube. To investigate the molecular pathogenesis of these tumors, we performed genomic profiling on a cohort of 31 adenomatoid tumors of the male and female genital tracts. We identified that all tumors harbored somatic missense mutations in the *TRAF7* gene, which encodes an E3 ubiquitin ligase belonging to the family of tumor necrosis factor receptor-associated factors (TRAFs). These mutations all clustered into one of five recurrent hotspots within the WD40 repeat domains at the C-terminus of the protein. Functional studies in vitro revealed that expression of mutant but not wildtype *TRAF7* led to increased phosphorylation of nuclear factor-kappa B (NF- κ B) and increased expression of L1 cell adhesion molecule (L1CAM), a marker of NF- κ B pathway activation. Immunohistochemistry demonstrated robust L1CAM expression in adenomatoid tumors that was absent in normal mesothelial cells, malignant peritoneal mesotheliomas, and multilocular peritoneal inclusion cysts. Together, these studies demonstrate that adenomatoid tumors of the male and female genital tract are genetically defined by *TRAF7* mutation that drives aberrant NF- κ B pathway activation.

Keywords

adenomatoid tumor; epididymis; fallopian tube; uterus; mesothelial cells; *TRAF7*; tumor necrosis factor alpha (TNF α); nuclear factor-kappa B (NF- κ B); L1CAM

Users may view, print, copy, and download text and data-mine the content in such documents, for the purposes of academic research, subject always to the full Conditions of use: http://www.nature.com/authors/editorial_policies/license.html#terms

To whom correspondence should be addressed: David A. Solomon, MD, PhD, Department of Pathology, University of California, San Francisco, 513 Parnassus Ave, Box 0102, Health Sciences West 451, San Francisco, CA 94143, Phone (415) 514-9761, Fax (415) 476-7963, david.solomon@ucsf.edu.

DISCLOSURES

The authors declare no competing financial interests related to this study.

INTRODUCTION

Adenomatoid tumors are the most common neoplasm of the epididymis where they typically present as small, painless extra-testicular masses in young or middle age adults and are often diagnosed after orchiectomy. Histologically similar tumors also arise in the uterus and fallopian tube, which are also called adenomatoid tumors given their presumed relatedness. Adenomatoid tumors in women are similarly found in young or middle age adults where they are most often discovered incidentally during hysterectomy or salpingectomy for other clinical indications such as endometrial cancer, ovarian cancer, or uterine leiomyomas. Apart from rare examples, adenomatoid tumors exhibit a benign clinical course without recurrence after resection and do not require additional therapy. Microscopically, they are poorly circumscribed neoplasms composed of a variable population of cuboidal to flattened cells with prominent cytoplasmic vacuolization arranged in cords with numerous cystically dilated spaces simulating vascular channels. The intervening stroma often contains abundant smooth muscle and elastic fibers and may have a prominent lymphocytic inflammatory infiltrate. Adenomatoid tumors of the male and female genital tract are presumed to be of mesothelial origin based on their morphological and ultrastructural features, as well as expression of markers typical of mesothelial cells and mesotheliomas including calretinin, WT1, D2-40, and cytokeratin.¹⁻⁶

The molecular pathogenesis of these relatively common tumors of the male and female genital tract is unknown. Of note is a growing number of case reports documenting an association of adenomatoid tumors arising in patients who are immunosuppressed for treatment of autoimmune disease or following allograft organ transplantation, and rare examples of immunosuppressed patients with giant or multiple adenomatoid tumors have also been reported.⁷⁻¹¹ This suggests a potential link between adenomatoid tumors and deregulated cytokine signaling pathways within mesothelial cells. Herein, we report the discovery of a defining genetic cause of adenomatoid tumors that may help to explain this association of adenomatoid tumors with immune dysregulation.

MATERIALS AND METHODS

Study population and tumor specimens

This study was approved by the Institutional Review Board of the University of California, San Francisco. Thirty one adenomatoid tumors from a cohort of 28 patients were retrieved from the pathology archives of our institution, spanning years 1994 to 2016. All tumor specimens had been fixed in 10% neutral-buffered formalin and embedded in paraffin. Paraffin embedded blocks of adjacent uninvolved testis, fallopian tube, or uterus were also retrieved for each patient. Pathologic review of all tumor samples was performed to confirm the diagnosis by N.M.J., K.G., J.T.R., C.Z., and D.A.S.

Targeted next-generation DNA sequencing and mutational analysis

Tumor tissue and uninvolved testis, fallopian tube, or uterus was macrodissected from formalin-fixed, paraffin-embedded blocks for the 28 patients. Genomic DNA was extracted from the macrodissected tissue using the QIAamp DNA FFPE Tissue Kit (Qiagen)

according to the manufacturer's protocol. Capture-based next-generation DNA sequencing was performed at the University of California, San Francisco Clinical Cancer Genomics Laboratory, using an assay that targets all coding exons of 479 cancer-related genes, select introns of 47 genes, and *TERT* promoter with a total sequencing footprint of 2.8 Mb (UCSF500 Cancer Panel; Supplemental Table 3).¹² Sequencing libraries were prepared from genomic DNA, and target enrichment was performed by hybrid capture using a custom oligonucleotide library (Roche NimbleGen). Sequencing was performed on an Illumina HiSeq 2500. Duplicate sequencing reads were removed computationally to allow for accurate allele frequency determination and copy number calling. The analysis was based on the human reference sequence (NCBI build 37) using the following software packages: BWA: 0.7.13, Samtools: 1.1 (using htslib 1.1), Picard tools: 1.97 (1504), GATK: Appistry v2015.1.1-3.4.46-0-ga8e1d99, CNVkit: 0.7.2, Pindel: 0.2.5b8, SATK: Appistry v2015.1.1-1-gea45d62, Annovar: v2016Feb01, Freebayes: 0.9.20, and Delly: 0.7.2.^{13–20} Single nucleotide variants and insertions/deletions were visualized and verified using Integrated Genome Viewer. Genome-wide copy number analysis based on on-target and off-target reads was performed by CNVkit and Nexus Copy Number (Biodiscovery).¹⁶

TRAF7 cDNA expression vector construction and site-directed mutagenesis

A human wildtype *TRAF7* cDNA (CCDS10461) with flanking 5' BamHI and 3' EcoRI restriction sites was synthesized by GenScript and cloned into the pCDF1-MCS2-EF1-Puro expression vector (System Biosciences). p.H521R, p.S561R, and Y538S mutations were engineered into the pCDF1-*TRAF7* construct by site-directed mutagenesis using the QuikChange II XL kit (Stratagene) as directed by the manufacturer. The coding sequence of all expression vectors was verified by Sanger sequencing. Primer sequences used for the mutagenesis reactions were as follows:

TRAF7 H521R Fwd: 5'-CTCACAGGCCTCAACCGCTGGGTGCGGGCCCTG-3'
 TRAF7 H521R Rev: 5'-CAGGGCCCGCACCCAGCGGTTGAGGCCTGTGAG-3'
 TRAF7 S561R Fwd: 5'-GACGTCTGGTGGCAGGGTCTACTCCATTGCTG-3'
 TRAF7 S561R Rev: 5'-CAGCAATGGAGTAGACCCTGCCACCAGACGTC-3'
 TRAF7 Y538S Fwd: 5'-CTGTACAGCGGCTCCTCCAGACAATCAAGATC-3'
 TRAF7 Y538S Rev: 5'-GATCTTGATTGTCTGGGAGGAGCCGCTGTACAG-3'.

Cell culture and transfections

293T cells were obtained directly from ATCC and were maintained in Dulbecco's Modified Eagle Medium (DMEM) supplemented with 10% fetal bovine serum at 37°C in 5% CO₂. Empty pCDF1 vector or pCDF1-*TRAF7* wildtype and mutant expression vectors were transfected into 293T cells using Fugene 6 (Roche) as described by the manufacturer.

Western blot

Protein was extracted from 293T cells in RIPA buffer at 48 hours after transfection, resolved by SDS-PAGE, and immunoblotted following standard biochemical techniques. Primary antibodies used were phospho-NF-κB p65 Ser536 (Cell Signaling, clone 7F1), total NF-κB

p65 (Cell Signaling, clone D14E12), L1CAM (Sigma, clone UJ127.11), and β -actin (Sigma, clone AC-15).

Immunohistochemistry

Immunohistochemistry was performed on whole formalin-fixed, paraffin-embedded tissue sections using anti-L1CAM antibodies (Sigma, clone UJ127.11) at a 1:1800 dilution following antigen retrieval. All immunostaining was performed in a Ventana Benchmark automated stainer. Diaminobenzidine was used as the chromogen, followed by hematoxylin counterstain. This immunohistochemistry was performed on 8 cases of adenomatoid tumor of the genital tract with confirmed somatic *TRAF7* mutation, 7 cases of normal mesothelial cells lining organs of the peritoneal cavity (4 from ovarian surface and 3 from fallopian tube surface), 7 cases of malignant peritoneal mesothelioma, and 6 cases of multilocular peritoneal inclusion cyst. All specimens were from the pathology archives of our institution and had been fixed in 10% neutral-buffered formalin and embedded in paraffin. We have previously reported the clinical, histopathologic, and molecular features for this cohort of malignant peritoneal mesotheliomas.¹²

RESULTS

Clinicopathologic features of the adenomatoid tumor patient cohort

In order to study the molecular pathogenesis of adenomatoid tumors of the male and female genital tracts, we assembled a cohort of matched tumor and normal tissue for 31 adenomatoid tumors from 28 patients for genomic analysis. The clinical features of this patient cohort are listed in Table 1. The 7 male and 21 female patients ranged in age from 31–72 years (median 47 years). The 7 male patients all had tumors located in the epididymis. The 21 female patients had tumors located in the fallopian tube (n=7) or uterus (n=17). The 7 male patients all underwent total or partial orchiectomy for a painless testicular mass. The majority of the tumors in the 21 females were discovered incidentally upon hysterectomy or salpingectomy for other pathologic processes or elective tubal ligation. Ten of the 25 patients (40%) with available clinical history had a history of immune dysregulation, which included autoimmune disease, HIV infection, or immunosuppressive medical therapy following allograft organ transplantation. Tumors ranged in size from 1 to 15 cm (mean 2.3 cm). One exceptional female (patient #14) who was immunosuppressed following heart and lung transplant for congenital heart disease underwent hysterectomy and bilateral salpingo-oophorectomy at age 60 years and was found to have multiple distinct adenomatoid tumors, with one in the fallopian tube and three in the uterus. Another exceptional female (patient #15) who had systemic lupus erythematosus and was on immunosuppressive therapy following kidney transplant underwent hysterectomy for a giant adenomatoid tumor of the uterus (15 cm). After a median follow-up of approximately 12 months, no patients in this cohort experienced disease recurrence.

Genomic analysis of adenomatoid tumors of the genital tract

Targeted next-generation sequencing was performed on genomic DNA isolated from the 31 tumors, as well as matched normal tissue, as described in the Methods. This identified somatic missense mutations in the *TRAF7* gene in all 31 tumors (Figs. 1–4, Supplemental

Table 1). Each tumor contained a single missense mutation in *TRAF7*, which encodes an E3 ubiquitin ligase and is a member of the family of tumor necrosis factor receptor-associated factors (TRAFs). The mutations all clustered into one of five hotspots located in the WD40 repeats at the C-terminus of the protein (Fig. 5). The most common mutation was p.S561R occurring in 13/31 tumors (42%) due to either a c.1683C>G (n=7) or c.1683C>A (n=6) substitution. The second most common mutation was p.H521R occurring in 11/31 tumors (35%) due to c.1562A>G substitution. Among the other seven tumors, three harbored p.Y538S mutation, three harbored p.Y577S, and one harbored p.L519P. These *TRAF7* missense mutations were verified to be somatic (i.e. tumor-specific) in all cases. The mutant allele frequency for the *TRAF7* variants ranged from 1–34%. Cases with the highest *TRAF7* mutant allele frequencies had genomic DNA isolated from areas histologically visualized to contain a high tumor cell content. Cases with the lowest *TRAF7* mutant allele frequency had genomic DNA that was isolated from tumors containing sparse tumor nuclei that were diffusely infiltrating the uterine myometrium. No chromosomal gains, losses, or copy-neutral loss of heterozygosity involving the *TRAF7* locus at chromosome 16p13.3 were identified in any of the tumors. Therefore, these data suggest that *TRAF7* mutation is likely a clonal heterozygous alteration in adenomatoid tumors (i.e. present in all tumor cells), indicating that it is probably an early or initiating event in tumorigenesis.

In addition to *TRAF7* mutation, 9/31 tumors (29%) contained somatic nonsynonymous mutations in at least one additional gene (Fig. 4, Supplemental Table 2). Two of the 31 tumors (6%) contained a frameshift mutation in *SETD2*, which encodes a histone methyltransferase with specificity for lysine-36 of histone H3 and is recurrently mutated in renal cell carcinomas and pediatric gliomas.^{21,22} Two tumors contained missense mutations in *LRP1B*, which encodes a lipoprotein receptor-related protein. Two tumors contained missense mutations in *MED12*, a transcriptional co-activator that is recurrently mutated in uterine leiomyomas and breast fibroadenomas.^{23,24} One of the two *MED12* mutations (p.L36R), found in a uterine adenomatoid tumor, localizes within an activating mutational hotspot that has been identified near the N-terminus of the protein. However, the possibility that this *MED12* mutation represents contamination by an adjacent leiomyoma is a distinct possibility. No other genes sequenced in this cohort of 31 adenomatoid tumors contained recurrent genetic alterations (Supplemental Table 3). No chromosomal gains, losses, or focal amplifications or deletions were identified in any of the 31 tumors (Supplemental Fig. 1).

Sequencing of the four separate adenomatoid tumors in patient #14 identified different somatic *TRAF7* mutations in each tumor, confirming that these anatomically distinct tumors were also genetically distinct (Fig. 6). No pathogenic alterations were identified in the germline of this immunosuppressed patient to account for the multiple adenomatoid tumors. In order to study potential intratumoral genetic heterogeneity, genomic DNA was isolated and sequenced from four different regions of the giant adenomatoid tumor in patient #15. All four regions contained the identical *TRAF7* and *LRP1B* somatic mutations, and no private alterations were identified in any of the four regions, indicating that the *TRAF7* and *LRP1B* variants were likely early or initiating events in this tumor.

***TRAF7* mutations drive aberrant NF- κ B pathway activation**

In order to study the functional effects of these recurrent *TRAF7* mutations, we generated an expression vector for wildtype *TRAF7*, as well as three of the most common mutations observed in adenomatoid tumors (p.H521R, p.S561R, and p.Y538S). As *TRAF7* belongs to the family of TNF receptor-associated factors that are known to regulate nuclear factor-kappa B (NF- κ B),²⁵ we hypothesized that these recurrent *TRAF7* mutations might cause adenomatoid tumors through deregulation of NF- κ B signaling. Upon transfection of mutant but not wildtype *TRAF7* into human embryonic 293T cells, we observed an increase in phosphorylation of the p65 subunit of NF- κ B (Fig. 7), a post-translational modification associated with activation of NF- κ B signaling.^{26,27} L1 cell adhesion molecule (L1CAM) is a known transcriptional target of NF- κ B and has emerged as a reliable surrogate marker for tumors with activated NF- κ B signaling.^{28,29} We observed a robust increase in levels of L1CAM protein in cells expressing mutant but not wildtype *TRAF7* (Fig. 7). We therefore considered the possibility that *TRAF7* mutations cause adenomatoid tumors of the genital tract by activation of NF- κ B signaling.

To further assess this hypothesis, we performed immunohistochemistry for L1CAM protein on a series of adenomatoid tumors, as well as normal mesothelium and two other tumors of mesothelial origin – malignant peritoneal mesothelioma and multilocular peritoneal inclusion cyst, also known as benign multicystic mesothelioma. We observed strong membranous staining for L1CAM in all adenomatoid tumors (n=8) (Fig. 8, Supplemental Fig. 2, Table 2). In contrast, no appreciable L1CAM staining was seen in normal mesothelial cells lining organs of the peritoneal cavity (n=7), nor was staining seen in malignant peritoneal mesotheliomas (n=7) or multilocular peritoneal inclusion cysts (n=6) (Fig. 8 and Supplemental Figs. 3 and 4). Together, these data suggest that *TRAF7* mutations lead to the development of adenomatoid tumors, at least in part, through activation of NF- κ B signaling.

DISCUSSION

Our study identifies a defining genetic alteration in adenomatoid tumors of the genital tract, which was uniformly present in epididymal, uterine, and fallopian tube tumors. Thus, in addition to morphologic and immunophenotypic similarities, adenomatoid tumors of the epididymis in males and fallopian tube and uterus in females also share a common genetic basis, and therefore are all likely to be a single tumor entity.

In addition to adenomatoid tumors of the genital tract, *TRAF7* mutations have been recently identified at high frequency in intraneural perineuriomas, a rare nerve sheath tumor derived from perineurial cells.³⁰ Additionally, *TRAF7* mutations have been identified in benign meningiomas, particularly those of the secretory variant and those located in the anterior skull base, where they uniformly occur with concurrent mutations in *KLF4*, *AKT1*, or *PIK3CA*.^{31,32} Alterations involving *KLF4*, *AKT1*, or *PIK3CA* were not identified in any of the 31 adenomatoid tumors in this cohort, indicating that adenomatoid tumors are genetically distinct from meningiomas harboring *TRAF7* mutations. Nevertheless, *TRAF7* mutations appear to genetically define a group of neoplasms arising from cells whose function is lining or wrapping around vital organs such as the brain, peripheral nerves, testis, uterus, and fallopian tube.

TRAF7 mutations have also been identified in a small subset (approximately 2%) of malignant mesotheliomas of the pleural cavity.³³ Whether these tumors instead represent misclassified adenomatoid tumors of the pleural cavity is a distinct possibility. Our recent genomic analysis of pathologically confirmed malignant mesotheliomas of the peritoneum did not identify any tumors harboring *TRAF7* mutation.¹² None of the adenomatoid tumors of the genital tract in the present cohort were found to harbor alterations in *BAP1*, *NF2*, or *CDKN2A* that characterize the vast majority of malignant mesotheliomas. As such, mesothelial tumors of the pleural, peritoneal, and other body cavities that are identified to harbor *TRAF7* mutation should strongly raise the possibility of an adenomatoid tumor, especially if alterations typical of malignant mesothelioma or other diagnostic entity are not present.

The *TRAF7* mutations identified in adenomatoid tumors in this study, as well as those found in meningiomas and intraneural perineuriomas,^{30–32} are all heterozygous missense mutations that cluster within a few mutational hotspots in the WD40 repeat domains at the C-terminus of the encoded TRAF7 protein. This genetic pattern of heterozygous missense mutations that cluster within a limited number of mutational hotspots is strongly suggestive that these are activating, gain-of-function mutations, as opposed to inactivating, loss-of-function events (which are typically truncating mutations scattered throughout a gene accompanied by loss of heterozygosity). Thus, *TRAF7* is very likely to function as an oncogene, rather than a tumor suppressor gene, in these tumor types.

The identification of *TRAF7* mutations as the genetic basis for adenomatoid tumors provides a potential explanation for why immune dysregulation may contribute to the development of these tumors. *TRAF7* encodes an E3 ubiquitin ligase that is a member of the family of tumor necrosis factor receptor-associated factors (TRAFs). This family of proteins has been implicated in regulation of a number of critical immunomodulatory signaling pathways involving NF- κ B, interferon-regulatory factors (IRFs), c-Jun N-terminal kinases (JNKs), and p38 mitogen-activated protein kinases.^{25,34} We hypothesize that immunosuppression causes an abnormal inflammatory state within mesothelial cells lining the peritoneal cavity that either causes selective pressure for the acquisition of activating *TRAF7* mutation or potentiates the oncogenic effect of *TRAF7* mutation once acquired, thereby promoting the formation of adenomatoid tumors. Although further studies are necessary to completely unravel the mechanisms by which *TRAF7* mutations lead to the development of intraneural perineuriomas, meningiomas, adenomatoid tumors, and perhaps other as-yet unidentified tumor types, our study provides the first evidence that activation of NF- κ B signaling is likely to be at least one of the mechanisms by which *TRAF7* mutations cause these specific tumor types.

Supplementary Material

Refer to Web version on PubMed Central for supplementary material.

Acknowledgments

This study was supported by NIH Director's Early Independence Award (DP5 OD021403) and the UCSF Physician-Scientist Scholar Program to D.A.S. We thank the UCSF Brain Tumor Research Center (supported by NIH SPORE grant P50CA097257) for assistance with L1CAM immunohistochemistry.

References

1. Nogales FF, Isaac MA, Hardisson D, et al. Adenomatoid tumors of the uterus: an analysis of 60 cases. *Int J Gynecol Pathol.* 2002; 1:34–40.
2. Sangoi AR, McKenney JK, Schwartz EJ, et al. Adenomatoid tumors of the female and male genital tracts: a clinicopathological and immunohistochemical study of 44 cases. *Mod Pathol.* 2009; 22:1228–1235. [PubMed: 19543245]
3. Ferenczy A, Fenoglio J, Richart RM. Observations on benign mesothelioma of the genital tract (adenomatoid tumor). A comparative ultrastructural study. *Cancer.* 1976; 37:1478–1484. [PubMed: 1260666]
4. Mackay B, Bennington JL, Skoglund RW. The adenomatoid tumor. Fine structural evidence for a mesothelial origin. *Cancer.* 1971; 27:109–115. [PubMed: 4099694]
5. Taxy JB, Battifora H, Oyasu R. Adenomatoid tumors. A light microscopic, histochemical, and ultrastructural study. *Cancer.* 1974; 34:306–316. [PubMed: 4277347]
6. Said JW, Nash G, Lee M. Immunoperoxidase localization of keratin proteins, carcinoembryonic antigen, and factor VIII in adenomatoid tumors. Evidence for a mesothelial derivation. *Hum Pathol.* 1982; 13:1106–1108. [PubMed: 6184302]
7. Livingston EG, Guis MS, Pearl ML, et al. Diffuse adenomatoid tumor of the uterus with a serosal papillary cystic component. *Int J Gynecol Pathol.* 1992; 11:288–292. [PubMed: 1399234]
8. Cheng CL, Wee A. Diffuse uterine adenomatoid tumor in an immunosuppressed renal transplant recipient. *Int J Gynecol Pathol.* 2003; 22:198–201. [PubMed: 12649678]
9. Bulent Tiras M, Noyan V, Suer O, et al. Adenomatoid tumor of the uterus in a patient with chronic renal failure. *Eur J Obstet Gynecol Reprod Biol.* 2000; 92:205–207. [PubMed: 10996682]
10. Acikalin MF, Tanir HM, Ozalp S, et al. Diffuse uterine adenomatoid tumor in a patient with chronic hepatitis C virus infection. *Int J Gynecol Cancer.* 2009; 19:242–244. [PubMed: 19396001]
11. Mizutani T, Yamamuro O, Kato N, et al. Renal transplantation-related risk factors for the development of uterine adenomatoid tumors. *Gynecol Oncol Rep.* 2016; 17:96–98. [PubMed: 27556063]
12. Joseph NM, Chen YY, Nasr A, et al. Genomic profiling of malignant peritoneal mesothelioma reveals recurrent alterations in epigenetic regulatory genes BAP1, SETD2, and DDX3X. *Mod Pathol.* 2017; 30:246–254. [PubMed: 27813512]
13. Li H, Durbin R. Fast and accurate long-read alignment with Burrows-Wheeler transform. *Bioinformatics.* 2010; 26:589–595. [PubMed: 20080505]
14. Li H, Handsaker B, Wysoker A, et al. The Sequence Alignment/Map format and SAMtools. *Bioinformatics.* 2009; 25:2078–2079. [PubMed: 19505943]
15. Broad Institute. Picard. <http://broadinstitute.github.io/picard/>
16. Talevich E, Shain AH, Botton T, Bastian BC. CNVkit: genome-wide copy number detection and visualization from targeted DNA sequencing. *PLoS Comput Biol.* 2016; 12:e1004873. [PubMed: 27100738]
17. Ye K, Schulz MH, Long Q, Apweiler R, Ning Z. Pindel: a pattern growth approach to detect break points of large deletions and medium sized insertions from paired-end short reads. *Bioinformatics.* 2009; 25:2865–2871. [PubMed: 19561018]
18. Wang K, Li M, Hakonarson H. ANNOVAR: functional annotation of genetic variants from high-throughput sequencing data. *Nucleic Acids Res.* 2010; 38:e164. [PubMed: 20601685]
19. Garrison E, Marth G. Haplotype-based variant detection from short-read sequencing. *arXiv 1207.3907v2 [q-bio.GN]*.
20. Rausch T, Zichner T, Schlattl A, et al. DELLY: structural variant discovery by integrated paired-end and split-read analysis. *Bioinformatics.* 2012; 28:i333–i339. [PubMed: 22962449]

21. Dalglish GL, Furge K, Greenman C, et al. Systematic sequencing of renal carcinoma reveals inactivation of histone modifying genes. *Nature*. 2010; 463:360–363. [PubMed: 20054297]
22. Fontebasso AM, Schwartzentruber J, Khuong-Quang DA, et al. Mutations in SETD2 and genes affecting histone H3K36 methylation target hemispheric high-grade gliomas. *Acta Neuropathol*. 2013; 125:659–669. [PubMed: 23417712]
23. Makinen N, Mehine M, Tolvanen J, et al. MED12, the mediator complex subunit 12 gene, is mutated at high frequency in uterine leiomyomas. *Science*. 2011; 334:252–255. [PubMed: 21868628]
24. Lim WK, Ong CK, Tan J, et al. Exome sequencing identifies highly recurrent MED12 somatic mutations in breast fibroadenoma. *Nat Genet*. 2014; 46:877–880. [PubMed: 25038752]
25. Xie P. TRAF molecules in cell signaling and in human diseases. *J Mol Signal*. 2013; 8:7. [PubMed: 23758787]
26. Lawrence T, Bebie M, Liu GY, et al. Ikkalpha limits macrophage NF-kappaB activation and contributes to the resolution of inflammation. *Nature*. 2005; 434:1138–1143. [PubMed: 15858576]
27. Mattioli I, Sebald A, Bucher C, et al. Transient and selective Nf-Kappa B p65 serine 536 phosphorylation induced by T cell costimulation is mediated by I Kappa B Kinase Beta and controls the kinetics of p65 nuclear import. *J Immunol*. 2004; 172:6336–6344. [PubMed: 15128824]
28. Parker M, Mohankumar KM, Punchihewa C, et al. C11orf95-RELA fusions drive oncogenic NF-kB signaling in ependymoma. *Nature*. 2014; 506:451–455. [PubMed: 24553141]
29. Figarella-Branger D, Lechapt-Zalcman E, Tabouret E, et al. Supratentorial clear cell ependymomas with branching capillaries demonstrate characteristic clinicopathological features and pathological activation of nuclear factor-kappaB signaling. *Neuro Oncol*. 2016; 18:919–927. [PubMed: 26984744]
30. Klein CJ, Wu Y, Jentoft ME, et al. Genomic analysis reveals frequent TRAF7 mutations in intraneural perineuriomas. *Ann Neurol*. 2017; 81:316–321. [PubMed: 28019650]
31. Clark VE, Erson-Omay EZ, Serin A, et al. Genomic analysis of non-NF2 meningiomas reveals mutations in TRAF7, KLF4, AKT1, and SMO. *Science*. 2013; 339:1077–1080. [PubMed: 23348505]
32. Reuss DE, Piro RM, Jones DT, et al. Secretory meningiomas are defined by combined KLF4 K409Q and TRAF7 mutations. *Acta Neuropathol*. 2013; 125:351–358. [PubMed: 23404370]
33. Bueno R, Stawiski EW, Goldstein LD, et al. Comprehensive genomic analysis of malignant pleural mesothelioma identifies recurrent mutations, gene fusions and splicing alterations. *Nat Genet*. 2016; 48:407–416. [PubMed: 26928227]
34. Zotti T, Scudiero I, Vito P, Stilo R. The emerging role of TRAF7 in tumor development. *J Cell Physiol*. 2017; 232:1233–1238. [PubMed: 27808423]

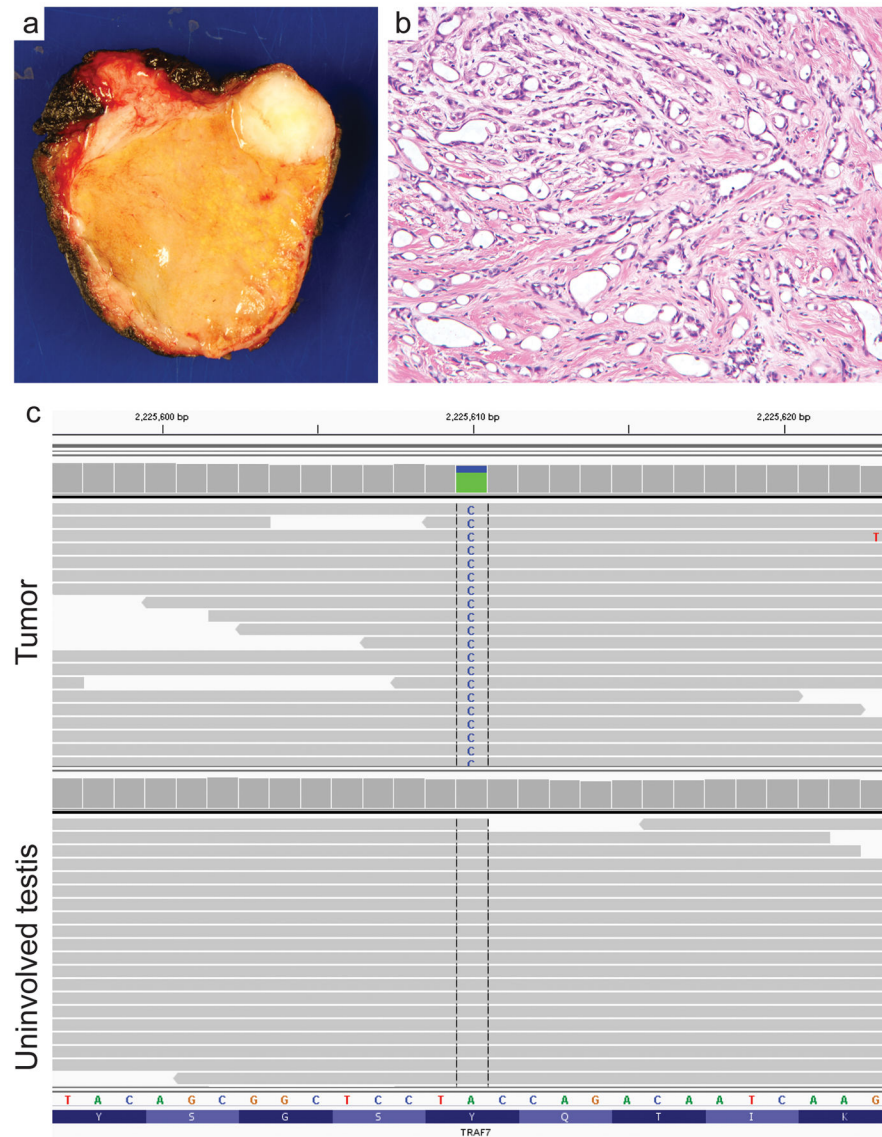


Figure 1.

Adenomatoid tumors of the epididymis are defined by somatic *TRAF7* mutations. (a) Gross photo from patient #1 showing a well-circumscribed nodule in the epididymis. (b) Hematoxylin and eosin (H&E) stained section of the tumor. (c) Next-generation sequencing reads from the tumor and adjacent uninvolved testis demonstrating a somatic *TRAF7* p.Y538S missense mutation.

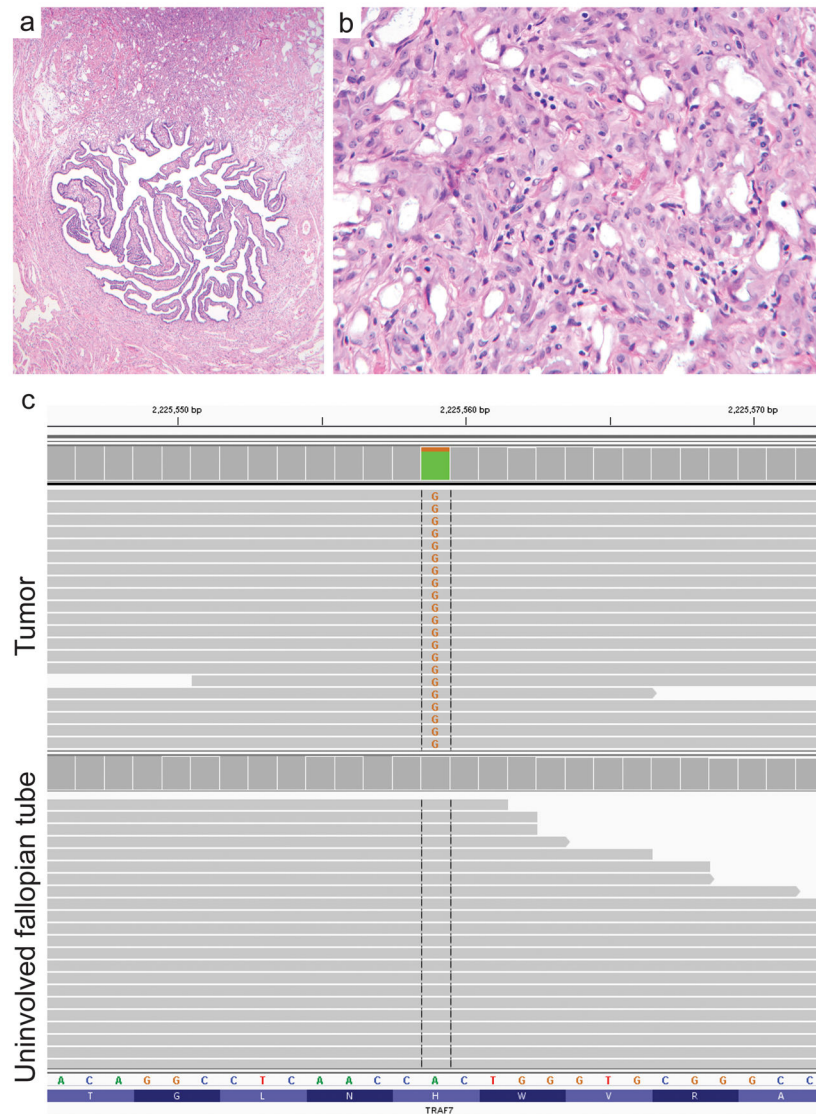


Figure 2. Adenomatoid tumors of the fallopian tube are defined by somatic *TRAF7* mutations. **(a)** Hematoxylin and eosin stained section from patient #12 showing an ill-defined lesion within the paratubal soft tissue. **(b)** H&E stained section of the tumor. **(c)** Next-generation sequencing reads from the tumor and adjacent fallopian tube epithelium demonstrating a somatic *TRAF7* p.H521R missense mutation.

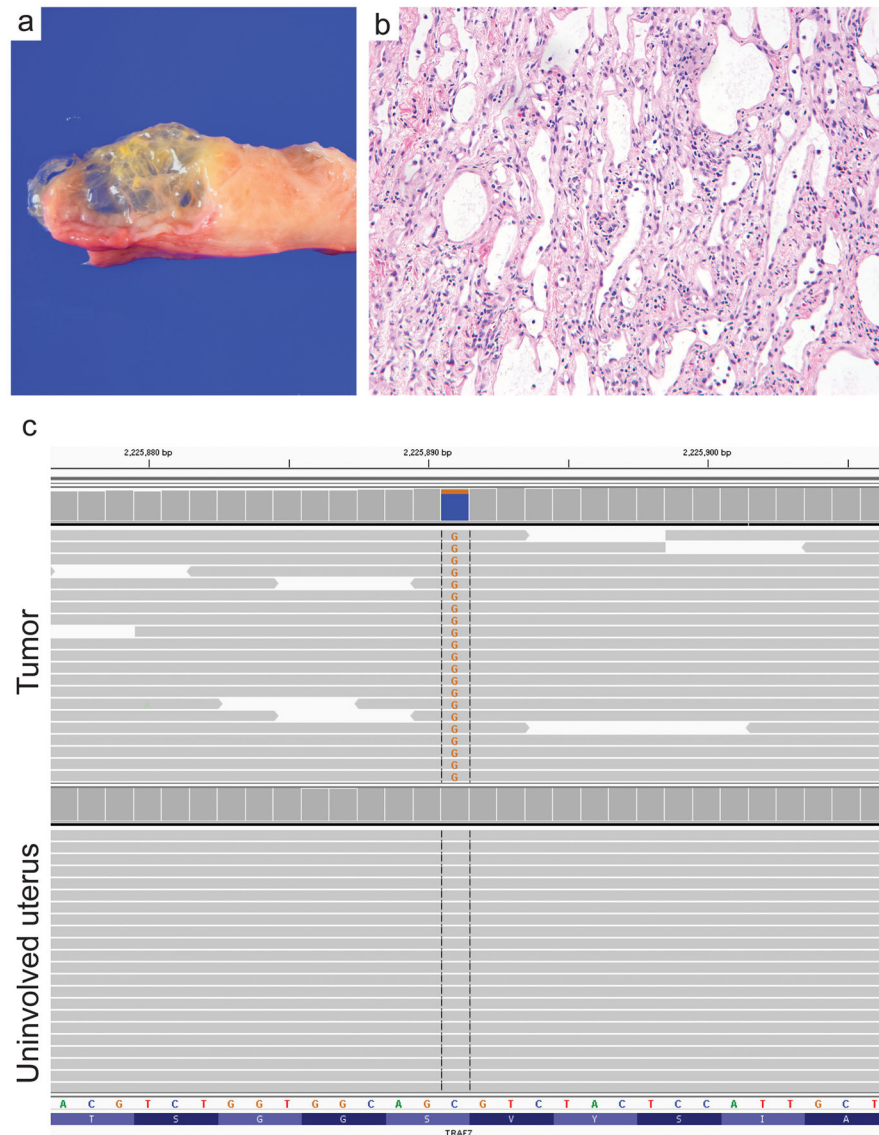


Figure 3.

Adenomatoid tumors of the uterus are defined by somatic *TRAF7* mutations. (a) Gross photo from patient #21 showing an ill-defined, yellow, multicystic lesion in the uterine body with extension into the broad ligament. (b) H&E stained section of the tumor. (c) Next-generation sequencing reads from the tumor and adjacent uninvolved uterus demonstrating a somatic *TRAF7*p.S561R missense mutation.

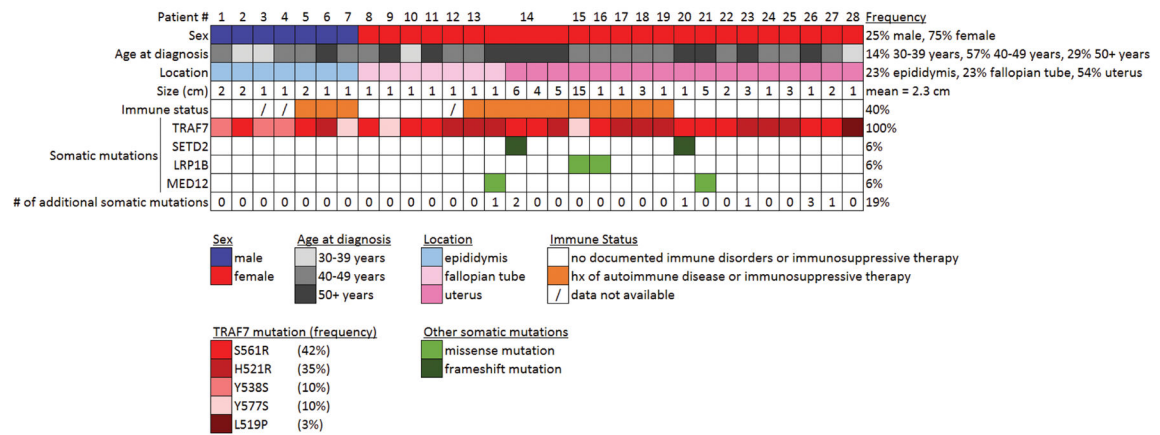


Figure 4. Genomic profiling results on 28 patients with adenomatoid tumors of the genital tract. Patient age, sex, immune status, tumor location, tumor size, *TRAF7* mutation, and other somatic mutations identified are shown.

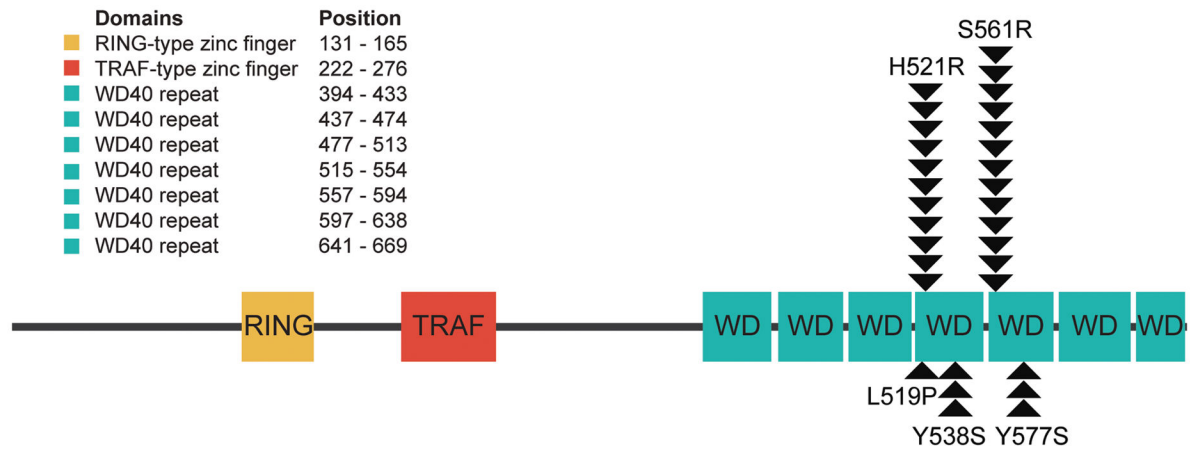


Figure 5.

Diagram of human TRAF7 protein with the location of the somatic missense mutations identified in the 31 adenomatoid tumors of the genital tract. The mutations all cluster within one of five recurrent hotspots in the C-terminal WD40 repeats.

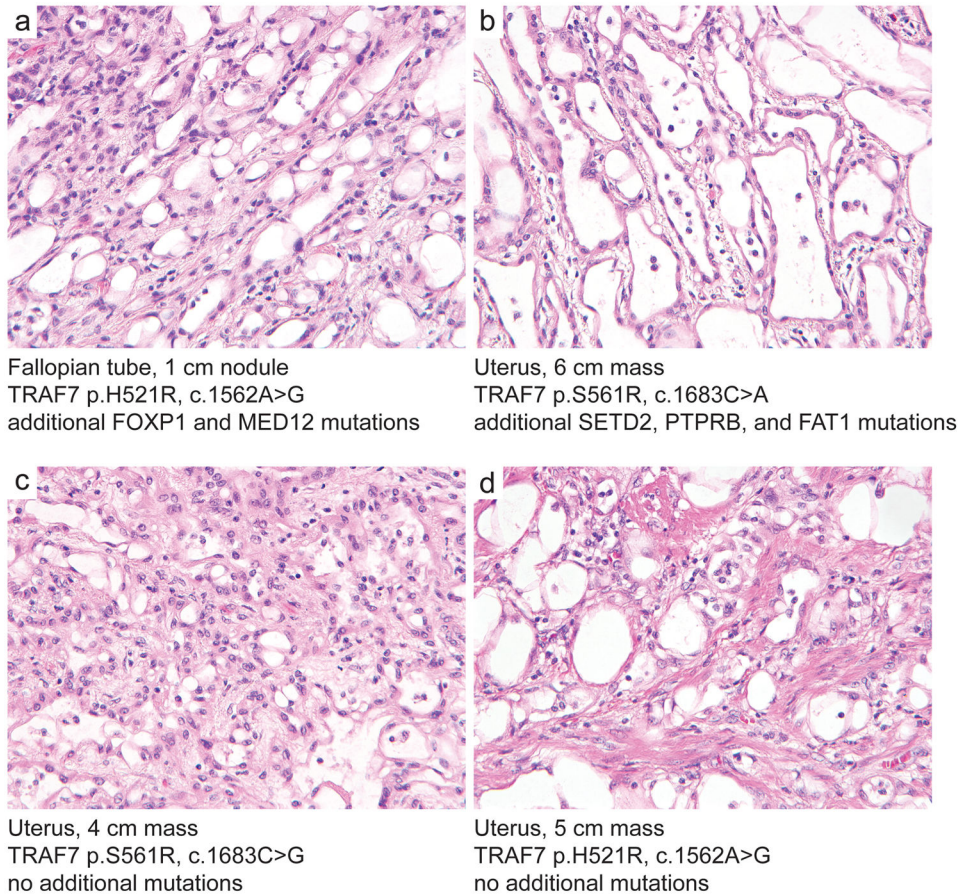


Figure 6.

Multiple anatomically and genetically distinct adenomatoid tumors of the uterus and fallopian tube in an immunosuppressed patient post-transplant. A 60 year old woman (patient #14) who was on immunosuppressive medical therapy following heart and lung transplant for congenital heart disease underwent hysterectomy and bilateral salpingo-oophorectomy for presumed uterine fibroids. Pathology instead revealed multiple adenomatoid tumors, one located in the right fallopian tube (**a**) and three located in the uterus (**b–d**). Genomic analysis identified distinct *TRAF7* mutations in each of the four tumors.

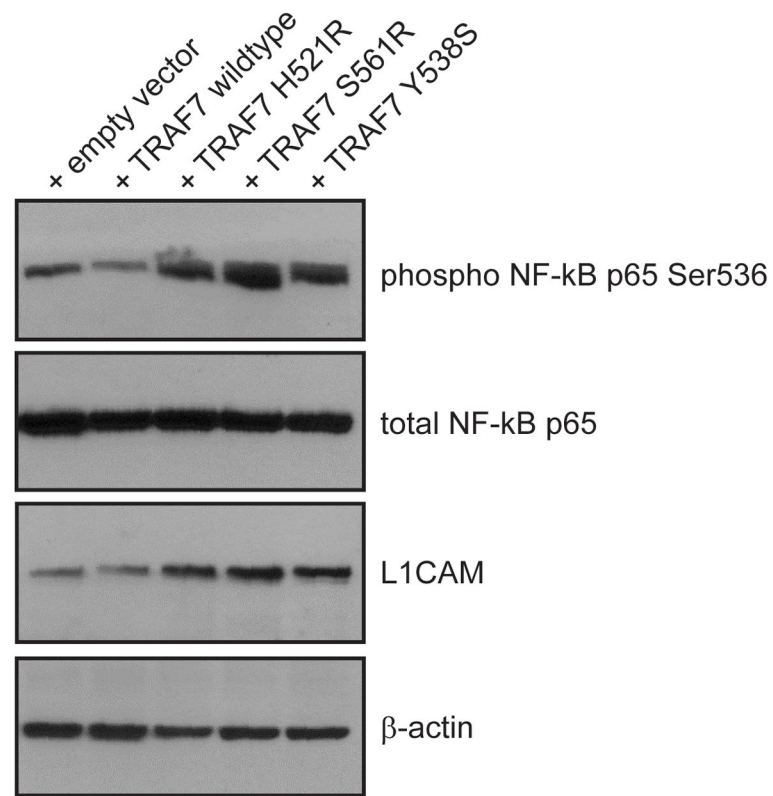


Figure 7. Western blots on total cell lysate from 293T cells after transfection with empty vector, wildtype *TRAF7*, or *TRAF7* harboring three different mutations recurrently found in adenomatoid tumors.

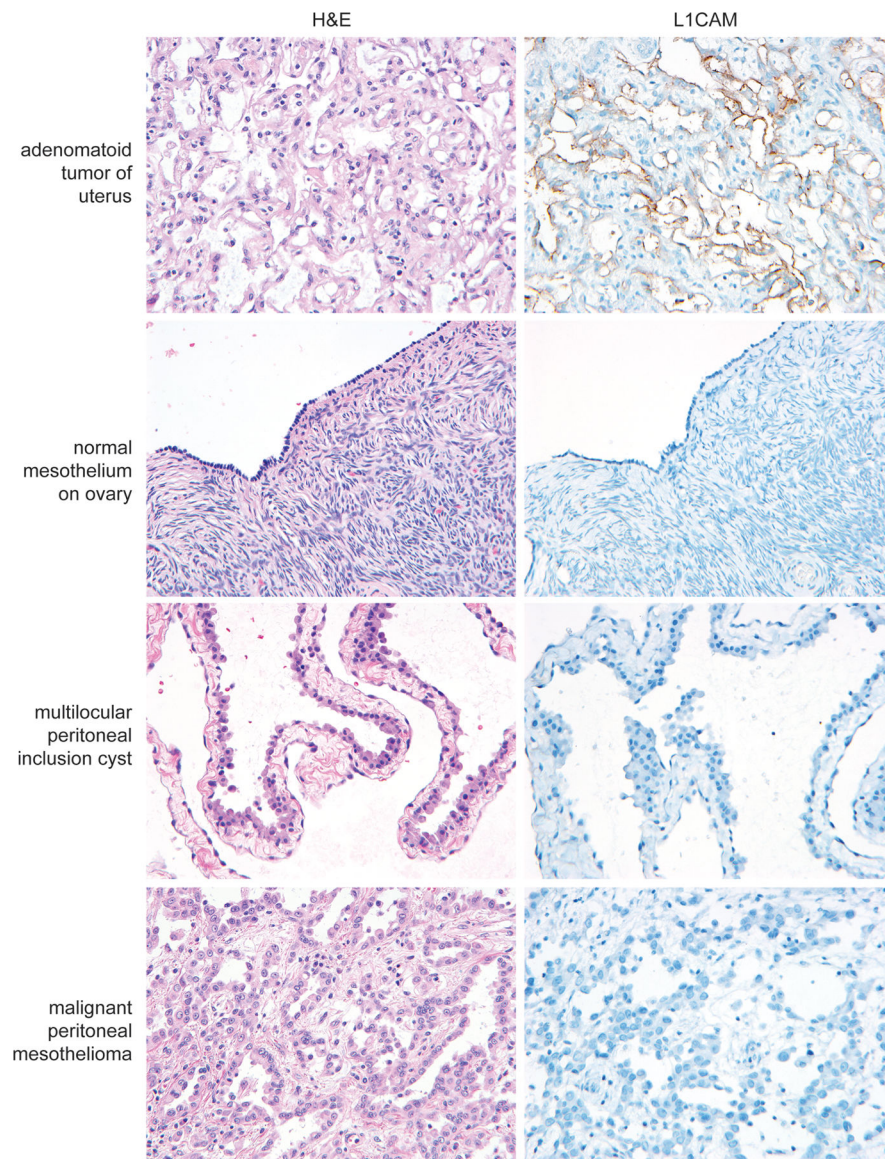


Figure 8. Immunohistochemistry for L1 cell adhesion molecule (L1CAM) demonstrates robust expression in adenomatoid tumors with the expected membranous staining pattern, whereas L1CAM expression is absent in normal mesothelial cells, malignant peritoneal mesotheliomas, and multilocular peritoneal inclusion cysts.

Table 1
Clinicopathologic and genetic features of the 28 patients with adenomatoid tumors of the male and female genital tracts.

Patient #	Age	Sex	Location	Indication for biopsy/resection	Hx of autoimmune disease or immunosuppression	Size (cm)	TRAF7 variant [†]	TRAF7 variant [†]	Sequencing reads over TRAF7 variant	Allele frequency for TRAF7 variant	Additional somatic mutations identified
1	43	M	Epididymis	testicular mass	None	2	p.Y538S	c.1613A>C	240	26%	-
2	31	M	Epididymis	testicular mass	None	2	p.S561R	c.1683C>A	120	18%	-
3	33	M	Epididymis	testicular mass	N/A	1	p.Y538S	c.1613A>C	187	17%	-
4	42	M	Epididymis	testicular mass	N/A	1	p.Y538S	c.1613A>C	151	7%	-
5	47	M	Epididymis	testicular mass	Immunosuppressed status post kidney and pancreas transplant	2	p.S561R	c.1683C>G	700	4%	-
6	70	M	Epididymis	testicular mass	Ankylosing spondylitis	1	p.H521R	c.1562A>G	415	5%	-
7	48	M	Epididymis	testicular mass	Ulcerative colitis, on immunosuppressive therapy	1	p.Y577S	c.1730A>C	250	11%	-
8	43	F	Fallopian tube	menorrhagia, uterine fibroids, and adnexal mass found to be hydrosalpinx with associated ipsilateral adenomatoid tumor	None	1	p.S561R	c.1683C>G	453	15%	-
9	53	F	Fallopian tube	uterine endometrioid adenocarcinoma	None	1	p.Y577S	c.1730A>C	1107	7%	-
10	35	F	Fallopian tube	elective tubal ligation	None	1	p.S561R	c.1683C>G	446	3%	-
11	72	F	Fallopian tube	ovarian fibrothecoma	None	1	p.S561R	c.1683C>G	518	1%	-
12	40	F	Fallopian tube	elective tubal ligation	N/A	1	p.H521R	c.1562A>G	160	8%	-
13	47	F	Fallopian tube	squamous cell carcinoma of the cervix	Grave's disease	1	p.H521R	c.1562A>G	524	12%	-
14	60	F	Fallopian tube and uterus	multiple adenomatoid tumors, paratubal (n=1) and myometrial (n=3)	Immunosuppressed status post heart and lung transplant	1, 6, 4, 5	p.H521R	c.1562A>G	253	21%	FOXP1 p.A279T, MED12 p.P1751L
							p.S561R	c.1683C>A	132	34%	SETD2 p.S587fs, PTPRB p.M1392V, FAT1 p.N760delinsMVYAVSGGN
							p.S561R	c.1683C>G	417	27%	-
							p.H521R	c.1562A>G	258	24%	-
15	42	F	Uterus	giant uterine adenomatoid tumor	Systemic lupus erythematosus, immunosuppressed status post kidney transplant	15	p.Y577S	c.1730A>C	268	32%	LRP1B p.A2354D
16	43	F	Uterus	menorrhagia and uterine fibroids	Mixed connective tissue disease, on immunosuppressive therapy	1	p.S561R	c.1683C>G	184	15%	LRP1B p.L509V
17	48	F	Uterus	symptomatic uterine fibroids	Grave's disease	1	p.H521R	c.1562A>G	348	9%	-

Patient #	Age	Sex	Location	Indication for biopsy/resection	Hx of autoimmune disease or immunosuppression	Size (cm)	TRAF7 variant [‡]	TRAF7 variant [‡]	Sequencing reads over TRAF7 variant	Allele frequency for TRAF7 variant	Additional somatic mutations identified
18	41	F	Uterus	menometrorrhagia and extensive adenomyosis	Immunosuppressed status post kidney transplant	3	p.H521R	c.1562A>G	127	11%	-
19	46	F	Uterus	menometrorrhagia and uterine fibroids	HIV infection	1	p.H521R	c.1562A>G	322	3%	-
20	57	F	Uterus	uterine endometrioid adenocarcinoma	None	1	p.S561R	c.1683C>G	981	4%	SETD2 p.K280fs
21	57	F	Uterus	dysmenorrhea and uterine adenomatoid tumor	None	5	p.S561R	c.1683C>A	200	12%	MED12 p.L36R
22	45	F	Uterus	uterine endometrioid adenocarcinoma	None	2	p.S561R	c.1683C>A	566	7%	-
23	55	F	Uterus	endometriosis and ovarian endometriotic cysts	None	3	p.H521R	c.1562A>G	183	3%	RAD50 p.Q1263R
24	47	F	Uterus	menorrhagia and uterine fibroids	None	1	p.H521R	c.1562A>G	212	3%	-
25	42	F	Uterus	endometriosis and ovarian endometriotic cysts	None	3	p.H521R	c.1562A>G	380	2%	-
26	59	F	Uterus	cervical dysplasia and uterine fibroids	None	1	p.S561R	c.1683C>A	307	8%	NUTM1 p.L949S, POL Q p.H225L, SPTA1 p.E486Q
27	49	F	Uterus	dysmenorrhea and uterine fibroids	None	2	p.S561R	c.1683C>G	540	18%	SPEN p.P2516A
28	37	F	Uterus	menorrhagia and uterine fibroids	None	1	p.L519P	c.1556T>C	465	3%	-

[‡] Annotated according to TRAF7 reference transcript NM_032271.

Table 2

L1CAM immunostaining results on normal mesothelium, adenomatoid tumors of the genital tract, and other mesothelial lesions of the peritoneal cavity.

Tissue	Cases with L1CAM immunostaining	Total number of cases	% positive for L1CAM
Normal mesothelium	0	7	0%
Adenomatoid tumor	8	8	100%
Malignant peritoneal mesothelioma	0	7	0%
Multilocular peritoneal inclusion cyst	0	6	0%